Article

Sequence Stratigraphy of the Jurassic Strata and Occurrences of Potential Sandstone Reservoirs in the ST Gas Field, Northern West Siberia Basin

Yefei Chen [1], Jinxiu Yang [2,3], Muhammad Talha [2], Ying Xia [2], Mingming Tang [2,3,]* and Rong Xie [2,3]

[1] Research Institute of Petroleum Exploration and Development, Beijing 100083, China; chenyefei@petrochina.com.cn
[2] Key Laboratory of Deep Oil and Gas, China University of Petroleum (East China), Qingdao 266580, China; yangjinxiu@upc.edu.cn (J.Y.); ls2101002@s.upc.edu.cn (M.T.); xiaying@s.upc.edu.cn (Y.X.); z22010093@s.upc.edu.cn (R.X.)
[3] School of Geosciences, China University of Petroleum (East China), Qingdao 266580, China
* Correspondence: tangmingming@upc.edu.cn

Abstract: Jurassic strata in the ST gas field of the northern West Siberia Basin have been regarded as a potential exploration target with undiscovered hydrocarbon resources. However limited research has been performed on the sequence stratigraphy of the Jurassic strata, as well as its sandstone distribution controlled by variable sea level change and sediment input. In this paper, four third-order sequences (SQ1, SQ2, SQ3, and SQ4) and nine fourth-order sequences for the Jurassic strata are interpreted based on seismic facies analysis and the lithology stacking patterns of seven wells. SQ1 is characterized by the special Bazhenov Formation which is featured by regionally distributed deep marine shales. SQ2 (J1) is composed of a coarsening upward sequence, the base of which is an unconformable surface that can be recognizable in both seismic profiles and well logging data. SQ3 (J2-J8) is composed of a complete fining-upward and coarsening-upward sequence, showing a series of transgressive and regressive successions. A complete SQ4 has not been drilled through by all the seven wells, only showing a coarsening upward succession on its top (J9) which evolves into a fining upward succession at the base of SQ3. Combined with the seismic inversion result, which predicts sandstone distribution, a sequence evolution model was built for SQ3 showing a full unit of transgressive system tract and highstand system tract (TST-HST) which often occurs in shallow marine shelves. During sequence development, most reservoir sandstones are deposited in the shelf and tidal delta environment at the bottom of the TST and the top of HST, and mudstones are deposited as shelf mudstones, especially at maximum flooding surface. That is controlled by both accommodation and sediment input. Generally, under this sequence framework, the depositional architecture can be further analyzed with implications for source rock, reservoir sandstones, and sealing rock, which may guide future gas exploration and exploitation in this area.

Keywords: sequence stratigraphy; Jurassic strata; sea level change; West Siberia; seismic

1. Introduction

ST is a giant gas field located in the north of the West Siberia Basin (Figure 1) [1,2]. Previous studies in this area often focus on post-Jurassic shallow marine to continental sandstone reservoirs which host most of the dry gas reserves. A lot has been done in terms of its tectonostratigraphic evolution [3,4], structural framework [5,6], stratigraphic sequence division and correlations [2,7], interpretation of the sedimentary facies and facies associations [8,9], as well as hydrocarbon accumulations [1,10–12]. However, limited research has been conducted on the underlying Jurassic strata which are expected to host potential oil and wet gas, and may represent future exploration and exploitation targets [1,2]. Therefore, we focused on the Jurassic strata in the ST gas field in this study by conducting

a comprehensive stratigraphic sequence analysis to build a sequence evolution model of Jurassic strata in order to facilitate future exploration.
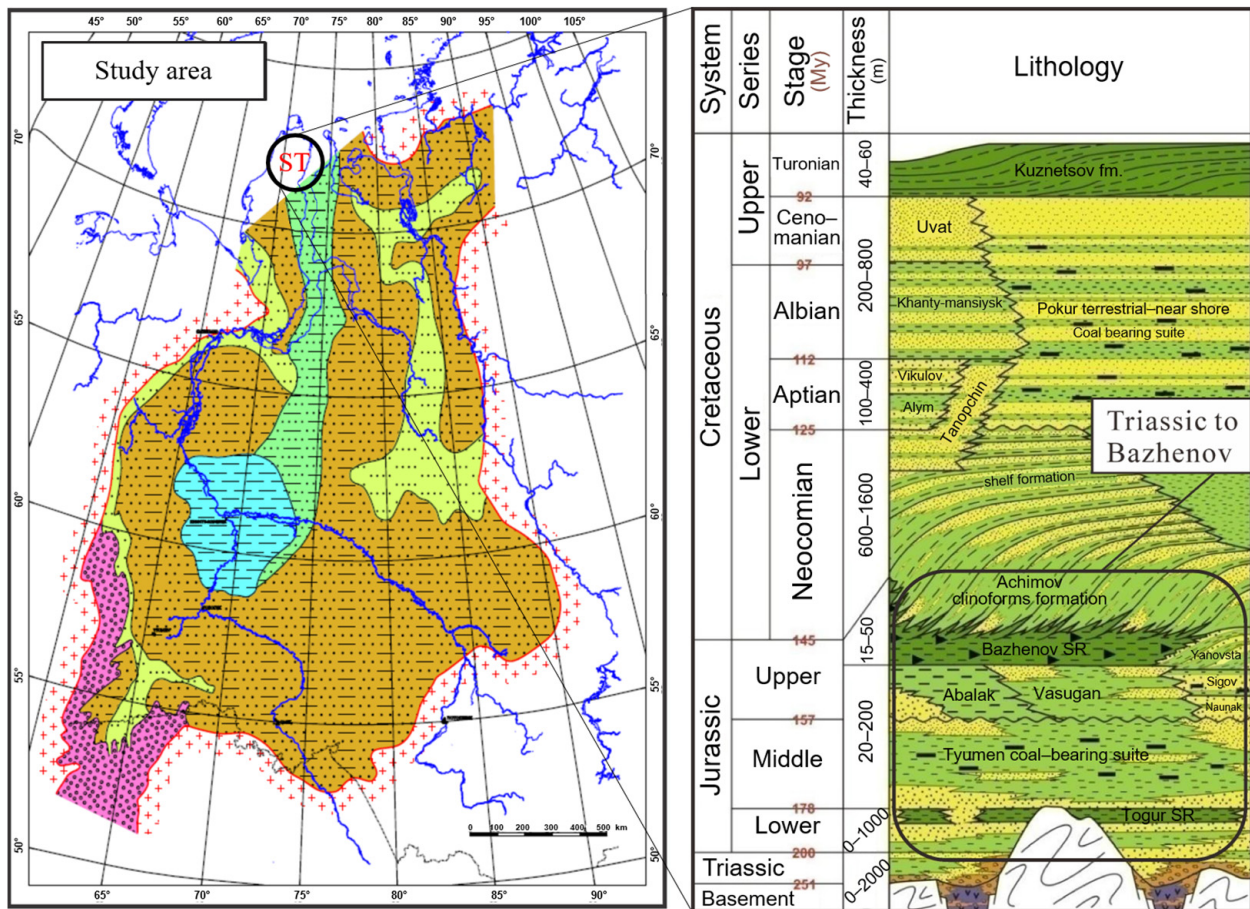
Figure 1. Location map (**left**) and lithostratigraphic log of Mesozoic strata (**right**) in northern West Siberia Basin. On the right, black bold dashes in the Middle Jurassic and Cretaceous correspond coal occurrence. Black triangles in Bazhenov Formation correspond organic matter.

Sequence stratigraphy deals with the characterization of genetically related strata, bounded by an unconformity surface or corresponding conformable surface [13]. The deposition of stratigraphic sequences is determined by factors like tectonic evolution, sea level change, and sediment supply [14,15]. By using well logging data, the vertical stacking patterns of Jurassic strata are analyzed to determine the lithologic successions which should be consistent with the sea level change [14,15]. Seismic profiles are also used to study the seismic characteristics of the sequence boundaries [16]. Guided by the theory of sequence stratigraphy, the sequence division and correlation can be carried out and a sequence framework can be built, which is the basis of further studies such as sedimentary facies and facies associations, as well as sedimentary models and the main types of reservoir sand bodies [17,18].

In this paper, the stratigraphic sequence framework of Jurassic strata is established using high-resolution sequence stratigraphy and correlation analysis of drill cores, well logs, and seismic sections from selected wells in the ST gas field. Furthermore, the sequence evolution model of the third-order sequence framework is developed on the basis of sequence division and correlation.

2. Geological Background

The West Siberia Basin (WSB) comprises three total petroleum systems (TPS), Bazhenov-Neocomian (upper Jurassic–lower Cretaceous), Togur-Tyumen (early to middle Jurassic),

and Northern West Siberian Mesozoic Composite TPS. The first two are oil-prone whereas the third one is mainly gas-prone. The ST gas field is situated in the northern part of WSB, more precisely in a peninsula adjacent to the Kara Sea (Figure 1). This region encompasses a complete sedimentary cover above the pre-Mesozoic basement (Figure 1), the environment of which transitioned from continental to transitional and to deep sea. Sedimentary thickness varies from 2 km to a maximum of 9 km [10]. Continental clastics of the Triassic Tampey series unconformably overlie the basement [19]. During the early to middle Jurassic, this study area underwent eustatic events to deposit lacustrine and estuarine siltstone and organic-rich shales of Togur and Radom members within the dominantly continental coal-bearing Tyumen Formation. These shale beds serve as hydrocarbon source rocks as well as seals between sandstone reservoirs within the Togur-Tyumen TPS [11,19]. Upper Jurassic evolved into marine shales of Abalak Formation which separates the Bazhenov-Neocomian and Togur-Tyumen TPS. Overlying is the upper Jurassic Bazhenov Formation which is organic-rich siliceous shale deposited widely in the whole basin under a deep-water anoxic environment. Bazhenov Formation is regarded as a principal source rock as it has generated more than 80% of the oil and gas for the WSB. Then, the basin was filled by the upper Jurassic Achimov Formation and Neocomian prograding clastic clinoforms, which form good stratigraphic traps above the Bazhenov source [5]. Although most of the discovered reserves are in structural traps, the stratigraphic traps in Jurassic-Neocomian are also promising and undiscovered [2]. Jurassic strata in most of the fields in northern WSB lie within the oil-condensate window, but the low hydrogen index, due to the increased thermal maturity calculated in the ST gas field, imparts gas-prone intervals in Jurassic strata [5,10]. Refs. [1,9] suggested that there may exist dry gas in Aptian-Cenomanian and wet gas in Jurassic-Neocomian sequences.

The West Siberia Basin is not only physically the world's largest petroliferous basin, but also produces more than 70% of Russia's oil [20,21]. Particularly, its northern part hosts Russia's huge gas reserves. Triassic to Paleogene sedimentary sequences are established on the Paleozoic and Precambrian basement [9]. Natural gas, condensate gas, and condensate oil fields were found in Jurassic-Cretaceous strata. Pre-Jurassic deposits and basement complexes are also promising [5]. In the south of the peninsula, the Lower-Middle Jurassic is alluvial lake facies, while shallow to deep marine deposits are available in the north and middle of the peninsula. The Late Jurassic organic-rich siliceous shales of the Bazhenov Formation were deposited in the whole study area under deep-sea conditions [10]. The structural shielding traps are developed in the Jurassic strata in the northwest active fault zone as a result of the local uplift. During the Late Jurassic (Callovian to Volgian), the basin experienced a big transgression. Therefore, the upper Jurassic sediments derived from high terrains of the southern WSB are the coarsest and most continental near the basement, while the Bazhenov Formation is the global maximum flooding surface, and the sediments show a fining upward feature (Figure 1). Sediments mainly come from the marine transgression period of the Upper Jurassic in the southeast, in a large-scale reducing environment, which is favorable for marine organic matter deposition [8]. Generally, the surface of the pre-Jurassic basement is similar to that of the Paleozoic basement. They gradually decrease from west to east, which is the same as the present surface of the pre-Jurassic basement, instead of forming a single dome [3].

3. Data and Methods

At present, there are three main criteria for sequence division in sequence stratigraphy. The first one is the classic type, presented by [22]. It is marked by the unconformity surface formed by the beginning and end of the sea level drop or its equivalent integration surface, emphasizing that the cause of the sequence unconformity interface is controlled by the rapid sea level drop. According to the degree of exposure of the shelf-slope break caused by the sea level drop amplitude and rate, the sequence interface is divided into two types: type I and type II sequence interfaces. The second one is the genetic stratigraphic sequence type, presented by [23]. It is marked by the maximum flooding surface as the interface between

the top and bottom of the sequence. This scheme fully emphasizes the instantaneous isochronism of the interface between the top and bottom of the sequence, while ignoring the division and correlation of other sedimentary bodies and even unconformities within the sequence. Third, the base-level cycle type is represented by [24]. It is considered that the stratigraphic base-level cycle is key to controlling the formation and division of stratigraphic sequences. The stratum datum level is restricted by sea level change, tectonic subsidence, sediment compensation, material supply rate, and sedimentary topography.

This study used geophysical well logs, drill cores, and seismic sections from seven selected wells (wells A, B, C, D, E, F, and G) in the ST gas field. The seismic data cover an area of ~1333 km^2. These data, along with the existing knowledge of Jurassic stratigraphic framework in the study area, theories of both classic and high-resolution sequence stratigraphy, fine stratigraphic division, and correlation technology, are all used to identify sequence boundary and flood surface; divide the third-, fourth-, and fifth-order sequences of a single well; delineate core and logging characteristics of each sequence; establish the well-seismic third- and fourth-order stratigraphic correlation framework; and define the evolution characteristics of "TST-HST" sequence of Jurassic strata.

Compared with shallower reservoirs, the reservoir quality in the deeper Jurassic strata is poorer and the lateral change is fast. Lithologic reservoirs with strong heterogeneity and thin interbeds are gradually becoming the main targets to replace reserves, and the difficulty of hydrocarbon exploration and development is increasing; especially the comprehensive popularization of horizontal wells puts forward higher requirements for fine reservoir prediction. The traditional inversion method is channel-by-channel, mainly considering the vertical variation of seismic amplitude (one-dimensional), but not the lateral variation of seismic waveform (three-dimensional). Moreover, it is a non-phased simulation algorithm with poor cross-well prediction. On the other hand, seismic waveform represents the tuning pattern of the vertical lithology combination of the reservoir, and its lateral change reflects the phase change characteristics of reservoir space, which is related to the sedimentary environment. Therefore, this study plans to adopt the method of "structural statistical representation driven by seismic waveform", and use the lateral change of waveform to represent the variability of reservoir spatial structure, which is more in line with the sedimentary geological law (Figure 2). Its main features include: (1) well simulation is constrained by the spatial variation information of seismic waveform, which creates a new high-resolution reservoir prediction method-well-seismic joint simulation, besides seismic inversion and well co-simulation, and realizes "phase-controlled" reservoir prediction; (2) using the high resolution of the well vertically and the high resolution of the seismic data horizontally, the vertical and horizontal precision of inversion can be improved at the same time; (3) it can widen the frequency band of inversion certainty and make the inversion result from completely random to gradually definite; and (4) the only inversion method in the industry that can adapt to uneven well location distribution is especially suitable for rolling evaluation. Therefore, based on the theory of waveform facies inversion, combining well and seismic data, this study conducted waveform facies inversion and simulation of the target formation, predicted the distribution characteristics of Jurassic sand bodies in three-dimensional space, and calculated the inversion sand thickness of different fourth-order sequences.
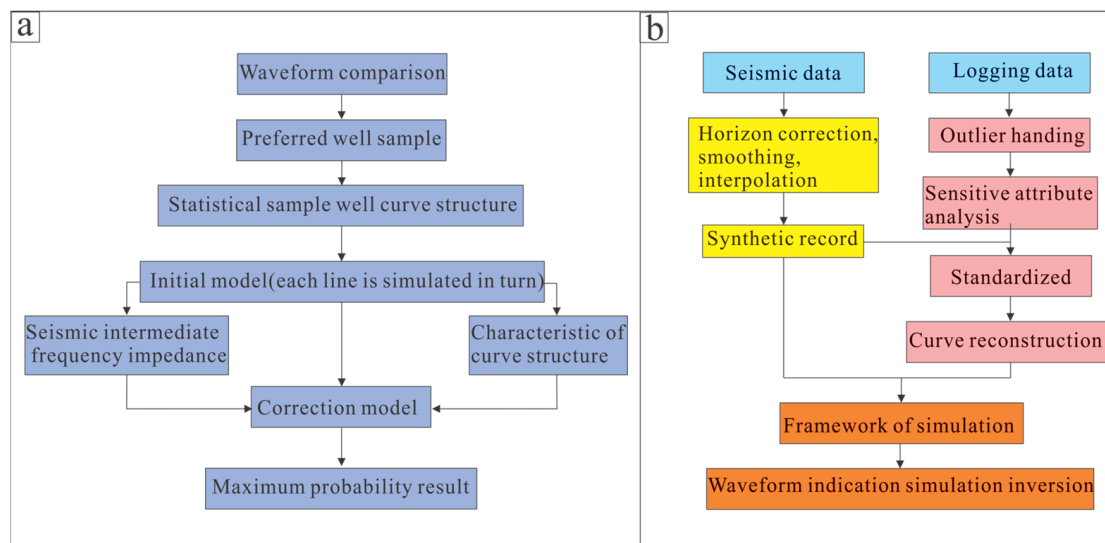
Figure 2. (**a**) algorithm idea and (**b**) seismic waveform indicates inversion process.

4. Establishment of Sequence Stratigraphic Framework in the Study Area

The establishment of a sequence stratigraphic framework in the study area of northern WSB mainly depends on core logging, well logging data, and the comprehensive analysis of seismic data, which has high reliability and can meet the requirements of sequence stratigraphic division.

4.1. Division Results of Single-Well Sequence Stratigraphy

The target strata in the study area include the Bazhenov Formation, Abalak Formation (J1), and Tyumen Formation (J2-9). According to the single-well sequence stratigraphic division results, the target strata are divided into four third-order sequences, namely SQ1, SQ2, SQ3, and SQ4 (Figure 3). SQ1 corresponds to the Bazhenov Formation and only develops a positive succession with the grain order narrowing upwards. This layer was formed in the maximum flooding period at the end of Jurassic and its lithology is mainly mudstone, with a thin thickness widely spread in the whole study area, which is considered as a high-quality source rock. The logging curve has the characteristics of low speed and high resistance, and the top and bottom have obviously high GR values. SQ2 corresponds to the Abalak Formation (J1) and only develops a reverse succession in which the grain order becomes coarser upward. The overall lithology is mainly sandstone with a small amount of mudstone. SQ3 is a complete sequence with a fining upward succession and coarsening upward succession, corresponding to most of the upper sections (J2-8) of the Tyumen Formation. The top and bottom of SQ3 are developed with high-quality sandstone mixed with thin mudstone, which is about 120 m thick, and the middle is developed with mudstone, showing a complete grain sequence cycle of transgression and regression (Figure 3). SQ4 corresponds to a small part of the lower member of Tyumen-3 (J9), and only one reverse cycle with coarsening grain order is developed, and a thin layer of high-quality sandstone mixed with mudstone is developed. SQ1 includes only one fourth-order sequence, namely SQ1-1. SQ2 includes two fourth-order sequences, namely SQ2-1 and SQ2-2. SQ3 includes five fourth-order sequences, namely SQ3-1, SQ3-2, SQ3-3, SQ3-4 and SQ3-5. SQ4 includes only one fourth-order sequence, namely SQ4-1.
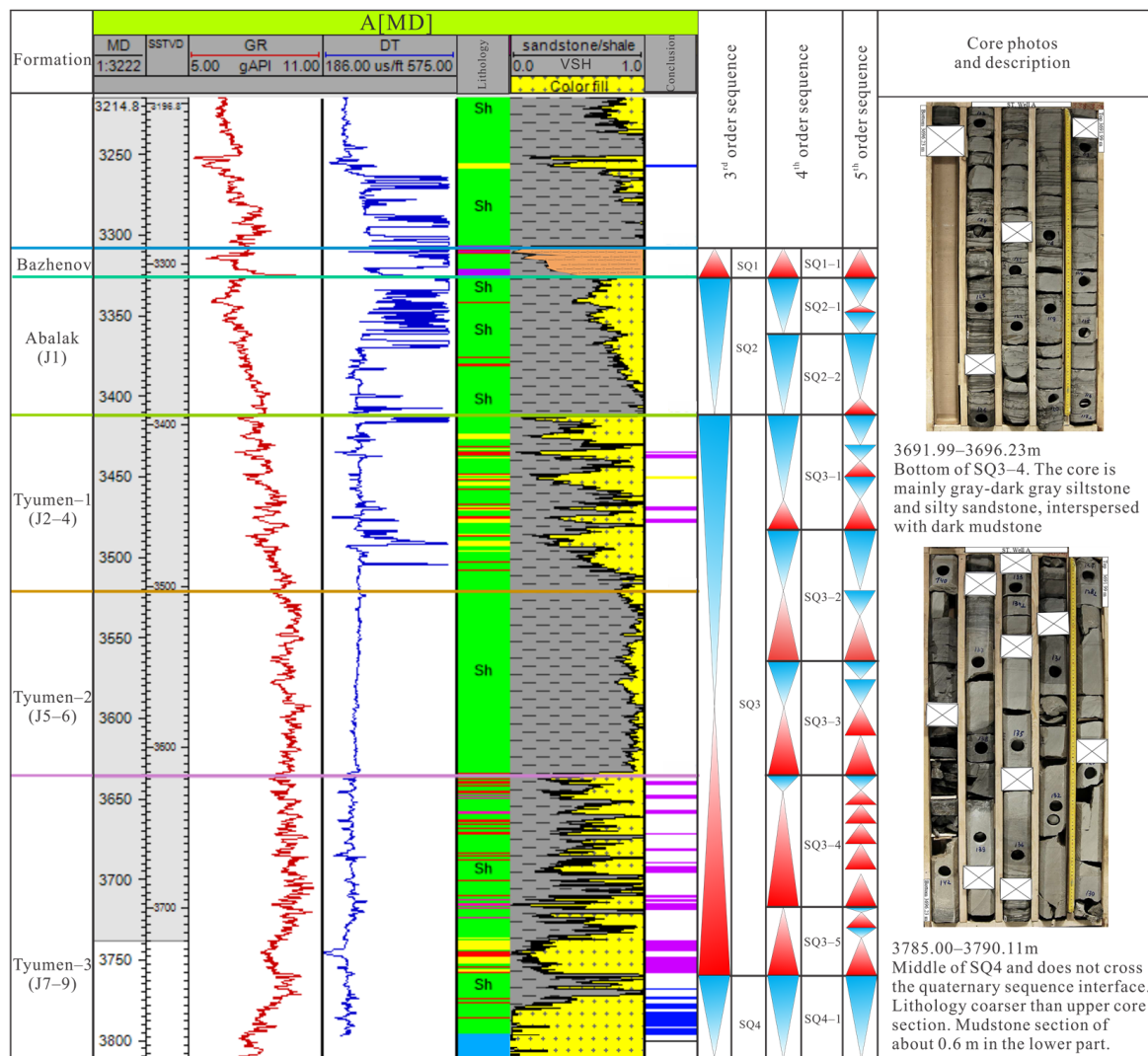
Figure 3. Sequence Stratigraphic column of well A*, showing the stacking patterns of the lithology indicated by different well loggings, as well as the key core features of sandstone reservoirs. Blue and red triangles correspond coarsening and fining upward sequence, respectively.

4.2. Establishment of Sequence Stratigraphic Framework

To establish the sequence stratigraphic framework, it is necessary to identify stratigraphic sequence interfaces at all levels within the study interval, including unconformity surfaces, sedimentary conversion surfaces, and large-scale flooding surfaces. The formation of sequence boundary represents the existence of erosion unconformity or sedimentary discontinuity with different scales. Its upper and lower sedimentary strata will produce some special responses in lithology, sedimentary facies combination, logging curve characteristics, and seismic reflection characteristics, which can be used independently or together as indicators to identify sequence boundaries. In seismic, the thickness of the third-order sequence has little change, showing good horizontal continuity.

According to the sedimentary characteristics of the drilling wells and related seismic characteristics of these boundaries, the high-resolution sequence stratigraphic framework of the study area is established in seismic and well ties to explore the stratigraphic characteristics of the target strata in the whole study area (Figures 4–8).
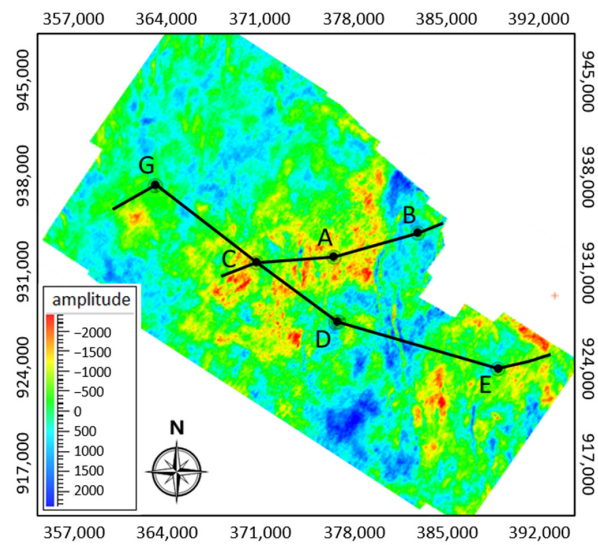
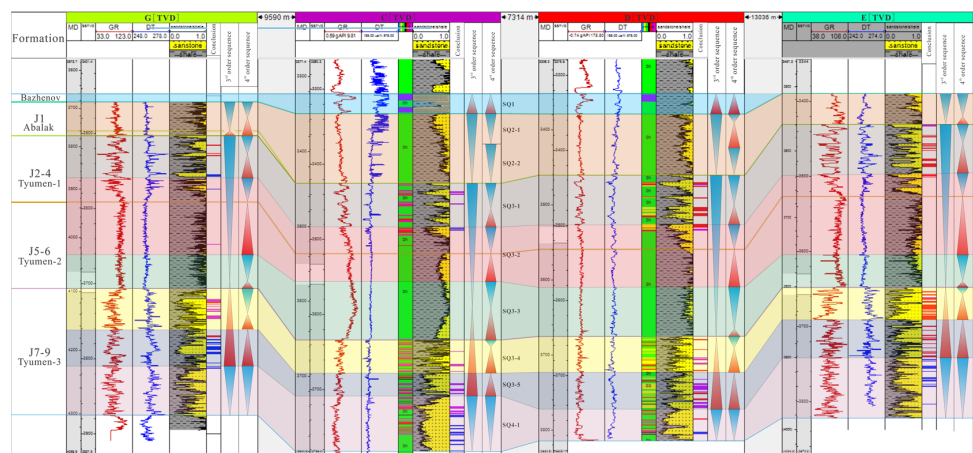**Figure 4.** RMS amplitude map of the top SQ3-4 showing the locations of the two well tie profiles.

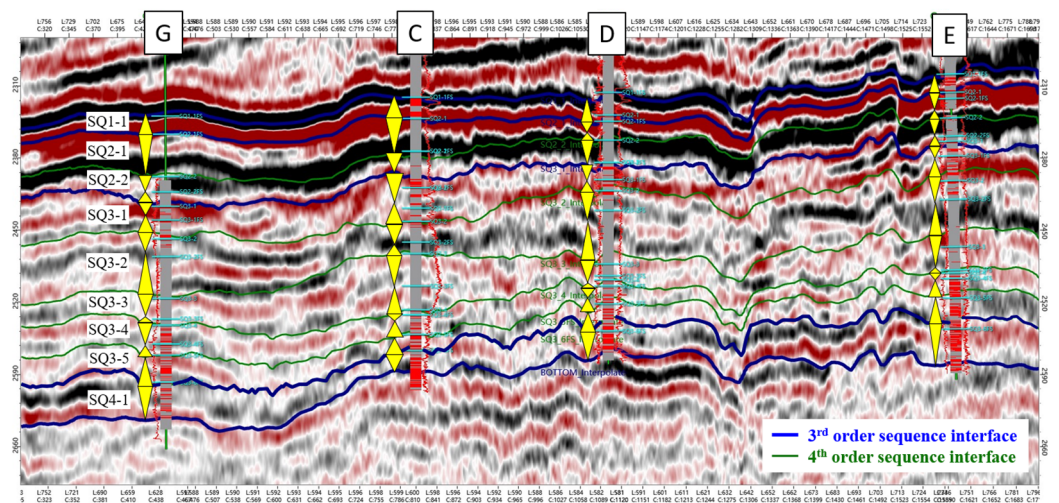**Figure 5.** Well tie profile showing the sequence correlation feature (G-C-D-E).

Figure 6. Well-seismic tie profile showing the sequence correlation feature (G-C-D-E).
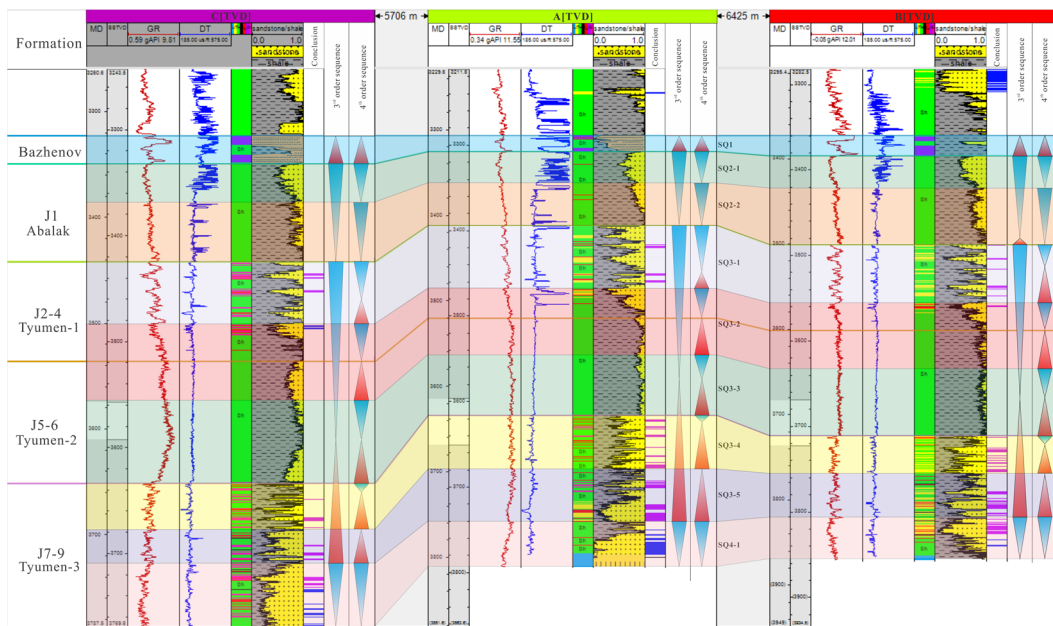
Figure 7. Well tie profile showing the sequence correlation feature (C-A-B).
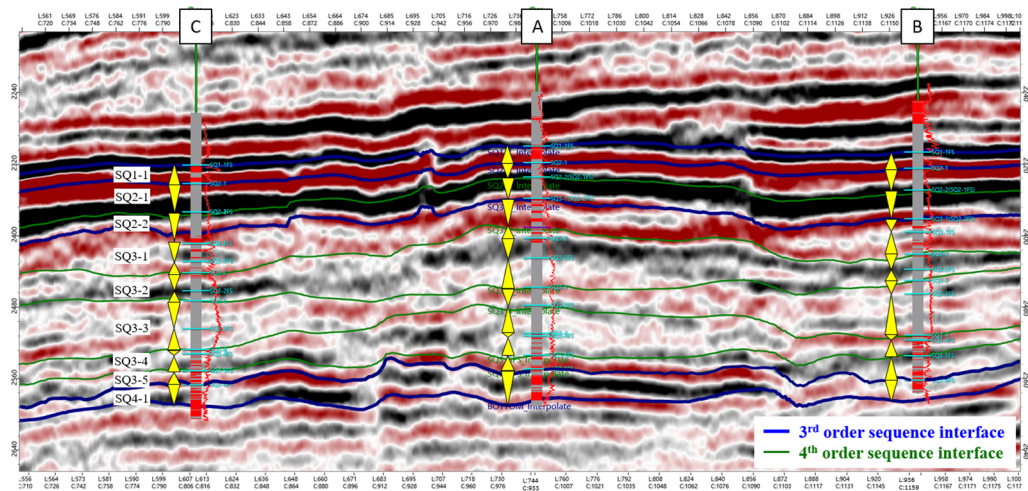

Figure 8. Well-seismic tie profile showing the sequence correlation feature (C-A-B).

Comparatively, the fourth-order sequences have great lateral changes (Figures 5–8). Specifically, the relationship between strata and the fourth sequence is as follows: Bazhenov: corresponds to the ascending half cycle of SQ1-1. J2-4: corresponds to the descending half cycle of the fourth sequences SQ3-1 and SQ3-2. J5-6: equivalent to the ascending half cycle and SQ3-3 of the fourth-order sequence SQ3-2. J7-8: equivalent to the fourth-order sequence SQ3-4 and SQ3-5. The drilling situation of SQ4-1 (J9) in each well is different, and the top interface is not uniform in a well-seismic correlation as some wells may not encounter J9.

5. Sandstone Prediction by Seismic Inversion

The sensitive density curve and shale content curve are used to simulate the waveform indication. The initial velocity is calculated by acoustic DT, the density is calculated by GGK density curve, and the zero-phase wavelet and the main frequency of 25 Hz are used for synthetic recording, based on which of the seismic calibration of key wells is carried out. The waveform characteristics of seismic records are in good agreement with synthetic records, and the correlation coefficient is higher (both above 0.58). The sensitivity of acoustic

DT and wave impedance is poor, which cannot effectively distinguish sandstone from mudstone (Figure 9). However, the GGK (density) and VSH (shale content) are sensitive to sand and mud, and, therefore, are used to predict the distribution of sand bodies.
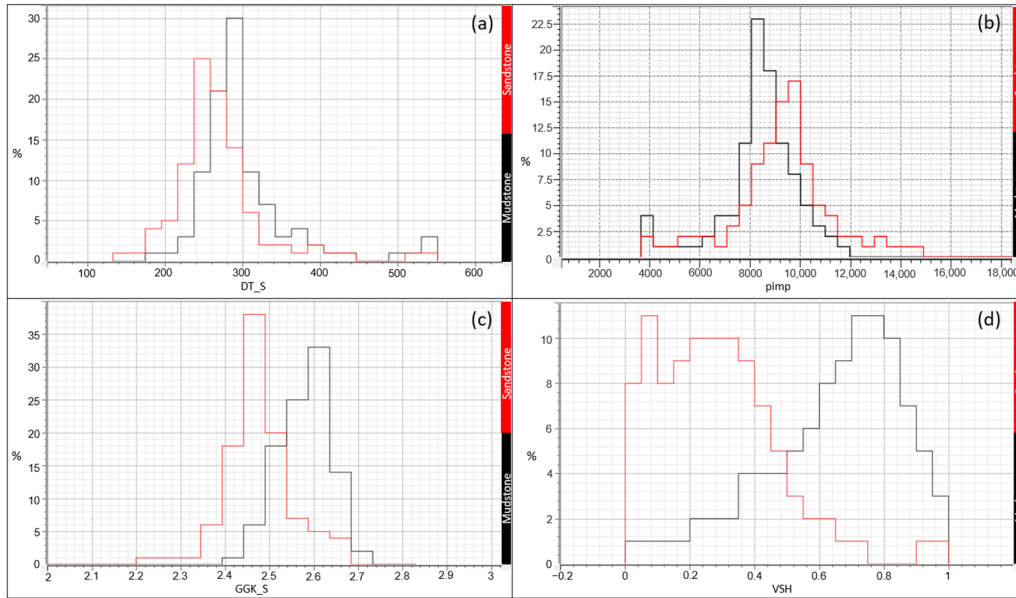

Figure 9. Sensitivity of acoustic DT (**a**), wave impedance (**b**), GGK (**c**), and VSH (**d**) to distinguish sandstone from mudstone.

The GGK parameter waveform simulation results show that sand bodies of SQ3-1 and SQ3-2 (J2-J4) and sand bodies of SQ3-4 and SQ3-5 (J7-J8) have relatively good prediction results. However, the sand body description effect of SQ4-1(J9) is not very accurate (Figure 10). Comparatively, the simulation results of the VSH parameter waveform indicate that the sand body distribution of the inversion body is in high agreement with the interpretation conclusion on the well, and the sand body distribution features that the sand bodies of SQ3-4, SQ3-5, and SQ4-1 are more developed than those of SQ3-1 and SQ3-2 (Figure 11). Both results show that the top and bottom of SQ3 developed good reservoir sandstones.
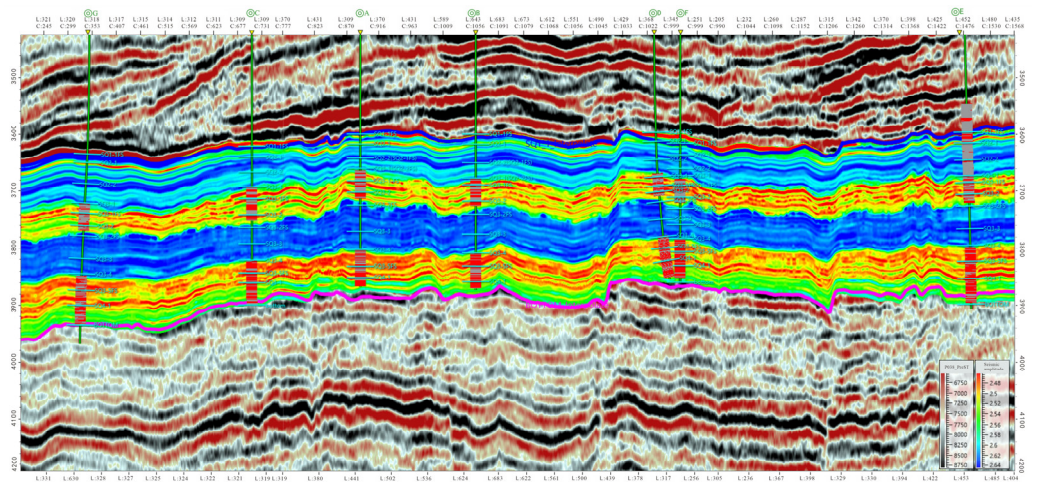

Figure 10. Well-seismic-tie profile showing the GGK simulation result with the red color indicating a high sandstone ratio (G-C-A-B-D-F-E).
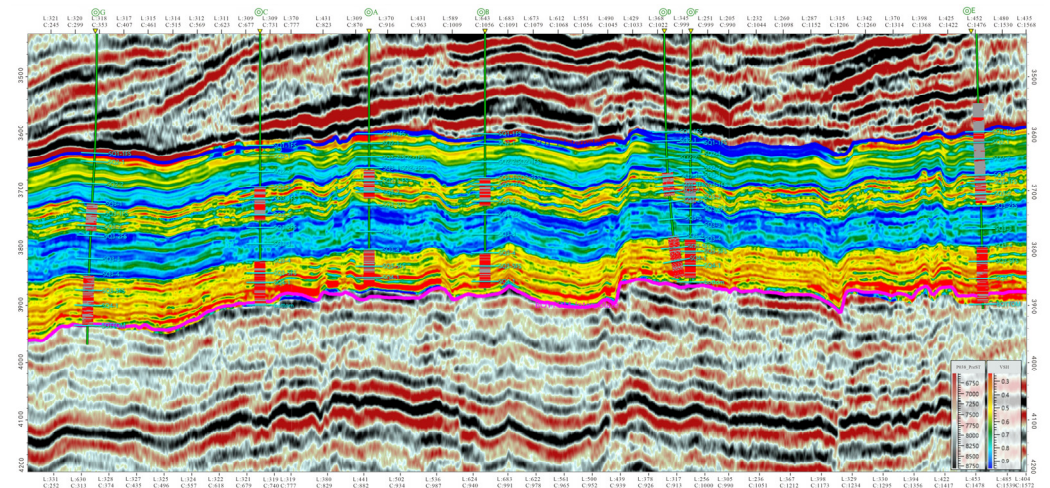
Figure 11. Well-seismic tie profile showing the VSH simulation result with the red color indicating a high sandstone ratio (G-C-A-B-D-F-E).

The average amplitude attribute and stratum thickness of all fourth-order sequences are extracted and compared with the results of the GGK density inversion and VSH shale content parameter inversion of the sand body thickness. The inversion thickness maps of the main sandstone reservoirs (SQ3-1, SQ3-2, SQ3-4, and SQ3-5) are made to show the sandstone distribution features of these fourth-order sequences (Figure 12).
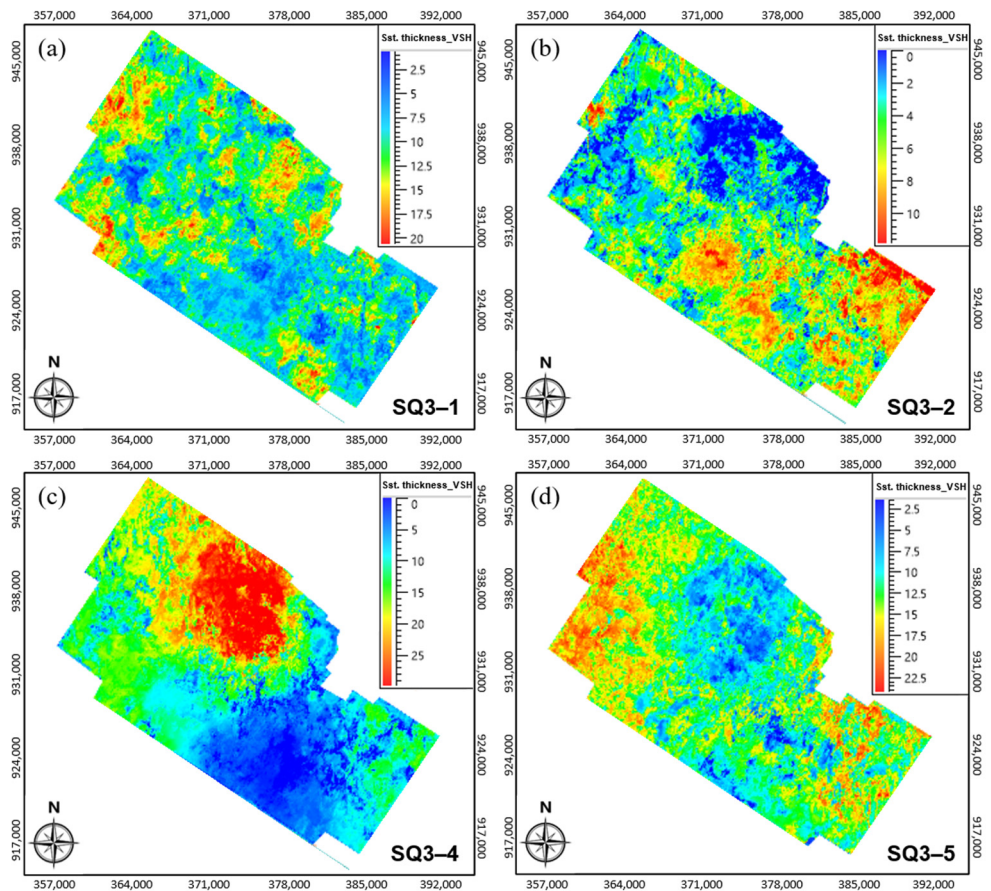
Figure 12. Inversion thickness maps of SQ3-1 (**a**), SQ3-2 (**b**), SQ3-4 (**c**), and SQ3-5 (**d**) based on VSH inversion.

SQ1-1: The average amplitude attribute is quite different from the inversion thickness of strata and sand bodies and the thickness of strata, probably because the overall amplitude of the seismic reflection layer here is strong. SQ1-1 sequence thickness is mainly between 13.4 and 51.3 m. The sand body inversion results of SQ1-1 show that the sequence sandstone is developed in the south of the study area.

SQ2-1: The average amplitude attribute is quite different from the stratum thickness, probably because the overall amplitude of the seismic reflection layer here is strong. SQ1 sequence thickness is mainly between 15 and 45 m. The inversion results of the GGK and VSH sand bodies in SQ1 are quite different, which may be related to the overall high-density value of this section, and its GGK curve baseline is higher than that of the J5-6 mudstone section.

SQ2-2: The average amplitude attribute shows that SQ2-2 has a strong amplitude in the north and southeast of the study area. The stratigraphic thickness map shows that the SQ2-2 sequence is thick in the east of the study area, and the sand body inversion results of SQ2-2 show that the sequence sandstone is well developed in the south and middle of the study area.

SQ3-1: The average amplitude attribute is consistent with the inversion thickness of the stratum and sand body and stratum thickness. The stratigraphic thickness map shows that the SQ3-1 sequence is thick in the north-central part of the study area. The inversion results of the GGK and VSH sand bodies of SQ1 are consistent, which shows that the sequence sandstone is well developed in the north-central part of the study area.

SQ3-2: The average amplitude attribute is consistent with the inversion thickness of the sand body and stratum thickness. The stratigraphic thickness map shows that the SQ3-2 sequence is thick in the south-central part of the study area. The GGK and VSH sand body inversion results of SQ3-2 are consistent, which shows that the sequence sandstone is well developed in the south-central part of the study area.

SQ3-3: The average amplitude attribute is different from the inversion thickness of the sand body and stratum thickness. The stratum thickness map shows that the SQ3-3 sequence is well developed in the middle of the study area. The GGK and VSH sand body inversion results of SQ3 are very consistent, which shows that the sequence sandstone is relatively undeveloped in the study area and only some sand bodies are developed in the central and western parts of the study area.

SQ3-4: The average amplitude attribute is different from the inversion thickness of the sand body and stratum thickness. The stratum thickness map shows that the SQ3-4 sequence is well developed in the north of the study area. The GGK and VSH sand body inversion results of SQ4 are very consistent, which shows that the sequence sandstone is well developed in the central and northern parts of the study area.

SQ3-5: The average amplitude attribute is different from the inversion thickness of the sand body and stratum thickness. The stratum thickness map shows that the SQ3-5 sequence is well developed on both sides of the study area. The inversion results of the GGK and VSH sand bodies of SQ5 are consistent with the distribution characteristics of the stratum thickness, which shows that the sequence sandstone is well developed on both sides of the study area.

SQ4-1: The average amplitude attribute is different from the inversion thickness of the sand body and stratum thickness. The stratum thickness map shows that the SQ4-1 sequence is well developed in the middle and south of the study area. The GGK and VSH sand body inversion results of SQ4-1 are very consistent, which shows that the sequence sandstone is well developed in the south of the study area.

6. Sequence Evolution Model

The geometry and lithology of the sequence stratigraphic units are controlled by four basic factors: tectonic subsidence, global sea level rise and fall, sediment supply rate, and climate change [25,26]. Among them, tectonic subsidence provides the accommodation space for sediment deposition. Secondly, global sea level change controls the distribution

pattern of strata and lithology. Lastly, the sediment supply rate, largely influenced by climate, controls the type and quantity of sediment, filling process, and ancient water depth in the basin [27]. The formation of sequence strata is mainly controlled by accommodation space (tectonic movement, global sea level rise and fall) and sediment supply. The establishment of the third-order sequence isochronous framework is mainly limited by sequence boundary (unconformity or disconformity) and flooding surface [28].

According to the relationship between the rate of sea level change and basin subsidence rate at the slope break zone of the sedimentary shoreline and the sequence boundary types, the marine sedimentary sequences can be divided into two types of third-order sequences [28,29], type I and type II. Type I sequence is composed of low-stand (LST), transgressive (TST), and highstand (HST) system tracts, and the bottom boundary of the sequence is a type I unconformity interface and its corresponding integration surface. Type II sequence is composed of a shelf margin system tract (SMST) and a transgressive (TST) and high-position (HST) system tract, and the bottom boundary of the sequence is the type II unconformity interface and its corresponding integration surface. The type-I sequence boundary is a regional unconformity interface, which is produced when the global sea level drops faster than the basin subsidence speed at the slope break of the sedimentary shoreline. Its upper and lower strata lithology, sedimentary facies, and strata occurrence can change greatly, and it has land exposure signs and deep valleys formed by river rejuvenation. Type II sequence boundary is formed when the global sea level decline rate is lower than the basin subsidence rate at the slope break zone of the sedimentary shoreline, so there is no relative sea level decline at this position, and, thus, there is a lack of regional erosion caused by river rejuvenation. The changes in lithology, sedimentary facies, and stratigraphic occurrence of the upper and lower strata are not as dramatic as those in Type I, but there is obvious accretion of overlying strata or the offshore shift towards the basin above the boundary.

Because the overall slope of the study area is extremely slow, the sequence boundary lacks obvious river rejuvenation and deep valley, and the lower system tract lacks basin floor fan and slope fan, so the third-order sequence in the study area consists of only a transgressive system tract (TST) and high-position system tract (HST) (Figure 13).
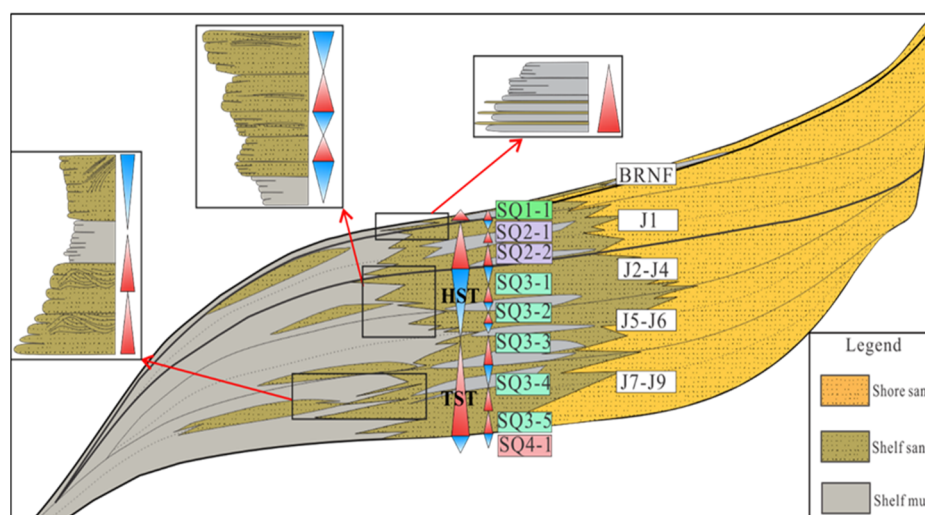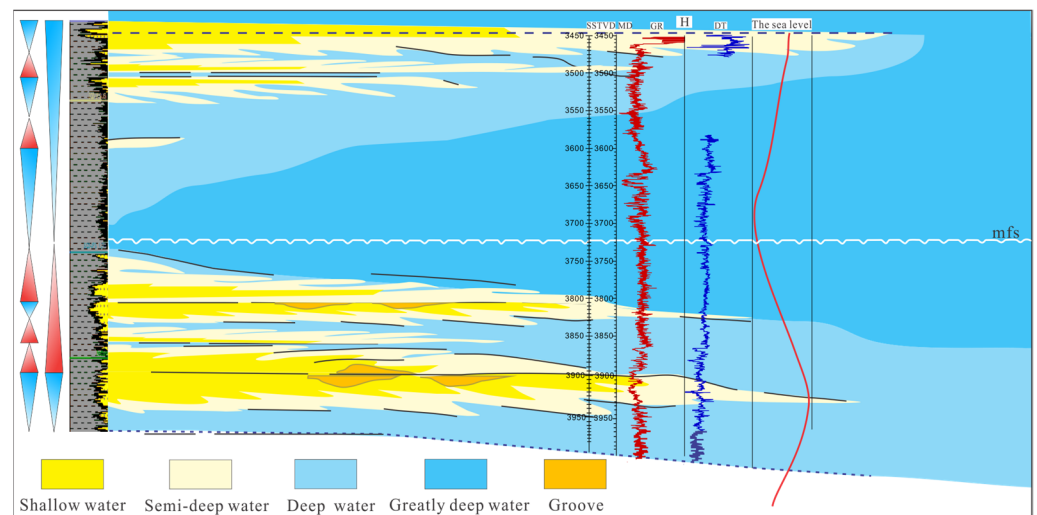

Figure 13. Sequence development model diagram.

The sequence boundary of this sequence development model is formed when the global sea level decline rate is lower than the basin subsidence rate at the slope break zone of the sedimentary shoreline, so there is no relative sea level decline at this position, and, thus, there is a lack of regional erosion caused by river rejuvenation. The changes in lithology, sedimentary facies, and stratigraphic occurrence of the upper and lower strata

are not drastic, but there is obvious accretion of overlying strata or the shift towards the basin on the coast above the boundary.

Therefore, tectonic subsidence controls the shape and provenance direction of the study basin and controls the boundary (unconformity) and development of the third-order sequence at the same time as the global third-order relative sea level change. The fourth-order relative sea level change simultaneously controls the boundary of the fourth-order sequence, its sedimentary environment, and sediment types. Based on the theory of sequence stratigraphy, comprehensive logging, core, and seismic data analysis, the vertical distribution model of the third- and fourth-order sequences of Jurassic strata in the study area is established (Figure 14).

Figure 14. Regional stratigraphic sequence development model of SQ3. 'mfs' = maximum flooding surface.

7. Conclusions

1. The development model of third-order sequence framework in the study area is established, providing a clear stratigraphic framework controlled mainly by sea level change, which is significant, along with seismic inversion, for understanding the sandstone reservoir distribution.
2. The target strata in the study area include the Bazhenov Formation, Abalak Formation (J1), and Tyumen Formation (J2-9), which are divided into four third-order and nine fourth-order sequences, namely SQ1 (Bazhenov), SQ2 (J1), SQ3 (J2-8), and SQ4 (J9).
3. GGK (density) and VSH (shale content) well logs, which are sensitive to sand and mud, are used to predict the distribution of sand bodies. The results show that the sand bodies of lower Tyumen (SQ3-4, SQ3-5, and SQ4-1) are more developed than those of upper Tyumen (SQ3-1 and SQ3-2).
4. A sequence evolution model was built showing a TST-HST sequence evolution pattern which often occurs in shallow marine shelves.

Author Contributions: Conceptualization, Y.C. and J.Y.; methodology, M.T. (Mingming Tang); validation, M.T. (Muhammad Talha), Y.X. and R.X. All authors have read and agreed to the published version of the manuscript.

Informed Consent Statement: Not applicable.

Data Availability Statement: The data presented in this study are available on request from the corresponding author. The data are not publicly available due to privacy.

Conflicts of Interest: The authors declare no conflict of interest.

References

1. Khafizov, S.; Syngaevsky, P.; Dolson, J.C. The West Siberian Super Basin: The Largest and Most Prolific Hydrocarbon Basin in the World. *Am. Assoc. Pet. Geol. Bull.* **2022**, *106*, 517–572. [CrossRef]
2. Schenk, C.J. *Geology and Assessment of Undiscovered Oil and Gas Resources of the Northern West Siberian Mesozoic Composite Total Petroleum System of the West Siberian Basin Province, Russia, 2008*; Moore, T.E., Gautier, D.L., Eds.; U.S. Geological Survey: Reston, VA, USA, 2018.
3. Kontorovich, V.A.; Ayunova, D.V.; Zakhryamina, M.O.; Kalinina, L.M. History of Upper Jurassic Reservoirs in Southeastern West Siberia (Case Study of Igol'sko-Talovoe Oilfield). *Russ. Geol. Geophys.* **2017**, *58*, 1240–1250. [CrossRef]
4. Vyssotski, A.V.; Vyssotski, V.N.; Nezhdanov, A.A. Evolution of the West Siberian Basin. *Mar. Pet. Geol.* **2006**, *23*, 93–126. [CrossRef]
5. Shuster, V.; Dziublo, A.; Shnip, O. Hydrocarbon Deposits in Non-Anticlinal Traps of the Yamal Peninsula of Western Siberia. *Georesursy* **2020**, *22*, 39–45. [CrossRef]
6. Surikova, E.S.; Solmin, A.E.; Guseva, S.M. Regional Model of the Geological Structure of the Yamal and Gydan Oil-and-Gas Areas. *IOP Conf. Ser. Earth Environ. Sci.* **2018**, *193*, 12067. [CrossRef]
7. Astakhova, A.A.; Birkle, E.A.; Bondarev, E.B. Sedimentological Analysis of TP1-TP5 Layers in the South Tambey Field Study Area, West Siberian Basin. In Proceedings of the 6th EAGE Saint Petersburg International Conference and Exhibition; European Association of Geoscientists & Engineers, Saint Petersburg, Russia, 7–10 April 2014; pp. 1–5.
8. TelnÆs, N.; Isaksen, G.H.; Douglas, A.G. A Geochemical Investigation of Samples from the Volgian Bazhenov Formation, Western Siberia, Russia. *Org. Geochem.* **1994**, *21*, 545–558. [CrossRef]
9. Ulmishek, G.F. Petroleum Geology and Resources of the West Siberian Basin, Russia. *U. S. Geol. Surv. Bull.* **2003**, *49*. [CrossRef]
10. Katz, B.J.; Robison, C.R.; Chakhmakhchev, A. Aspects of Hydrocarbon Charge of the Petroleum System of the Yamal Peninsula, West Siberia Basin. *Int. J. Coal Geol.* **2003**, *54*, 155–164. [CrossRef]
11. Kontorovich, A.; Moskvin, V.I.; Bostrikov, O.I.; Danilova, V.P.; Fomin, A.N.; Fomichev, A.S.; Kostyreva, E.A.; Melenevsky, V.N. Main Oil Source Formations of the West Siberian Basin. *Pet. Geosci.* **1997**, *3*, 343–358. [CrossRef]
12. Zhang, X.; Wang, H.; Ma, F.; He, Z.; Bai, B.; Liang, Y. Characteristics and Resource Potential of Jurassic Tight Shale Oil Reservoirs in West Siberian Basin. *Oil Gas Geol.* **2016**, *37*, 101–108, 116.
13. Zhu, X.M. *Sequence Stratigraphy*; China University of Petroleum Press: Qingdao, China, 2000; pp. 42–43.
14. Haq, B.U.; Hardenbol, J.; Vail, P.R. Chronology of Fluctuating Sea Levels Since the Triassic. *Science* **1987**, *235*, 1156–1167. [CrossRef] [PubMed]
15. Jervey, M.T. Quantitative Geological Modeling of Siliciclastic Rock Sequences and Their Seismic Expression. In *Sea-Level Changes: An Integrated Approach*; Special Publications of SEPM: Claremore, OK, USA, 1988; pp. 47–69. ISBN 9781565760899.
16. He, J.; Peng, B.; Li, L.; Tian, T.; Wu, Q. Carbonate Sedimentary Facies Analysis Based on Seismic Data—With the Example of Permian Changxin Formation in Some Area. *J. Chongqing Inst. Sci. Technol.* **2013**, 4–8.
17. Cui, B.W.; Zhang, S.; Fu, X.L.; Su, Y.X.; Jin, M.Y. Organic Sequence Stratigraphic Division and Its Influencing Factors' Analyses for Gulong Shale in Songliao Basin. *Pet. Geol. Oilf. Dev. Daqing* **2021**, *40*, 13–28.
18. Wang, J.T.; Chen, S.H.; Xu, J.L. Comprehensive Evaluation of Reservoirs in the Lin'an Region, Northwestern Zhejiang Based on Logging Data. *Acta Geol. Sichuan* **2022**, *42*, 101–108, 116.
19. Surkov, V.S. Rift Genesis and Oil-Gas Basins of Siberia. *Pet. Geol. Q. J.* **1998**, *33*, 394–399.
20. Lodewijkx, M.; Ingram, V.; Willemse, R. *West Siberia Oil Industry Environmental and Social Profile*; IWACO: Rotterdam, The Netherlands, 2001.
21. Chakhmakhchev, A.; Sampei, Y.; Suzuki, N. Geochemical Characteristics of Oils and Source Rocks in the Yamal Peninsula, West Siberia, Russia. *Org. Geochem.* **1994**, *22*, 311–322. [CrossRef]
22. Vail, P.R. Seismic Stratigraphy Interpretation Procedures. In *Atlas of Seismic Stratigraphy*; Bally, A.W., Ed.; AAPG Studies in Geology: Tulsa, OK, USA, 1987; pp. 1–10.
23. Galloway, W.E. Genetic Stratigraphic Sequences in Basin Analysis I: Architecture and Genesis of Flooding-Surface Bounded Depositional Units1. *Am. Assoc. Pet. Geol. Bull.* **1989**, *73*, 125–142. [CrossRef]
24. Cross, T. High-Resolution Stratigraphic Correlation from the Perspective of Base-Level Cycles and Sediment Accommodation. In Proceedings of the Northwestern European Sequence Stratigraphy Congress; Elsevier: Holland, The Netherlands, 1994; pp. 105–123.
25. Catuneanu, O.; Zecchin, M. High-Resolution Sequence Stratigraphy of Clastic Shelves II: Controls on Sequence Development. *Mar. Pet. Geol.* **2013**, *39*, 26–38. [CrossRef]
26. Hammes, U.; Frébourg, G. Haynesville and Bossier Mudrocks: A Facies and Sequence Stratigraphic Investigation, East Texas and Louisiana, USA. *Mar. Pet. Geol.* **2012**, *31*, 8–26. [CrossRef]

27. Wang, G.; Zhu, T.; Wang, H.; Wu, J.; Du, W.; Feng, D.; Wang, R. Integrated Sequence Stratigraphic Division and Vertical Distribution Characteristics of Marine Shale: A Case Study of the Wufeng Formation-Long-Maxi Formation in Southeastern Sichuan Basin. *Acta Sedimentol. Sin.* **2019**, *37*, 330–344.

28. Haiying, H.; Jun, W.; Guosheng, Q.; Xiaowei, S.; Yichang, Y.; Haiyang, S.; Yang, G.; Rui, G. Sequence Stratigraphic Framework and Sedimentary Evolution of the Cretaceous in Southern Iraq. *Earth Sci. Front.* **2023**, *30*, 122–138.

29. Holz, M.; Vilas-Boas, D.B.; Troccoli, E.B.; Santana, V.C.; Vidigal-Souza, P.A. Chapter Four—Conceptual Models for Sequence Stratigraphy of Continental Rift Successions. In *Advances in Sequence Stratigraphy*; Montenari, M., Ed.; Academic Press: Cambridge, MA, USA, 2017; Volume 2, pp. 119–186. ISBN 2468-5178.